Title	Giant Hysteretic Single-Molecule Electric Polarisation Switching above Room Temperature
Author(s)	Kato, Chisato; Machida, Ryo; Maruyama, Rio; Tsunashima, Ryo; Ren, Xiao-Ming; Kurmoo, Mohamedally; Inoue, Katsuya; Nishihara, Sadafumi
Citation	Angewandte Chemie International Edition , 57 (41) : 13429 - 13432
Issue Date	2018-10-08
DOI	10.1002/anie.201806803
Self DOI	
URL	https://ir.lib.hiroshima-u.ac.jp/00049752
Right	© 2018 Wiley-VCH Verlag GmbH & Co. KGaA, Weinheim This is the peer reviewed version of the following article: C. Kato, R. Machida, R. Maruyama, R. Tsunashima, X.-M. Ren, M. Kurmoo, K. Inoue, S. Nishihara, Angew. Chem. Int. Ed. 2018, 57, 13429., which has been published in final form at https://doi.org/10.1002/anie.201806803. This article may be used for non-commercial purposes in accordance with Wiley Terms and Conditions for Use of Self-Archived Versions. This is not the published version. Please cite only the published version. この論文は出版社版ではありません。引用の際には出版社版をご確認、ご利用ください。
Relation	

Giant Hysteretic Single-Molecule Electric Polarisation Switching above Room Temperature

Chisato Kato,[a] Ryo Machida,[a] Rio Maruyama,[a] Ryo Tsunashima,[b] Xiao-Ming Ren,[c],[d] Mohamedally Kurmoo,[e],[f] Katsuya Inoue,[a],[f],[g] Sadafumi Nishihara*[a],[f],[g]

Abstract: Continual progress has been achieved in information technology through unrelenting miniaturisation of the single memory bit in integrated ferromagnetic, ferroelectric, optical, and related circuits. However, as miniaturisation is approaching its theoretical limit, new memory materials are being sought as replacements. Here, we report a unique material exhibiting single-molecule electric polarisation switching that can operate above room temperature. The phenomenon occurs in a Preyssler-type polyoxometalate (POM) cluster we call a single-molecule electret (SME), which exhibits all the characteristics of ferroelectricity but without long-range dipole ordering. The SME affords bi-stability due to the two potential positions of localisation of a terbium ion (Tb^{3+}) trapped within the enclosed POM, which results in extremely slow relaxation of the polarization and electric hysteresis with high spontaneous polarisation and coercive electric fields. Our findings suggest that SMEs can potentially be applied to ultrahigh-density memory[1] and other molecular-level electronic devices operating above room temperature.[2]

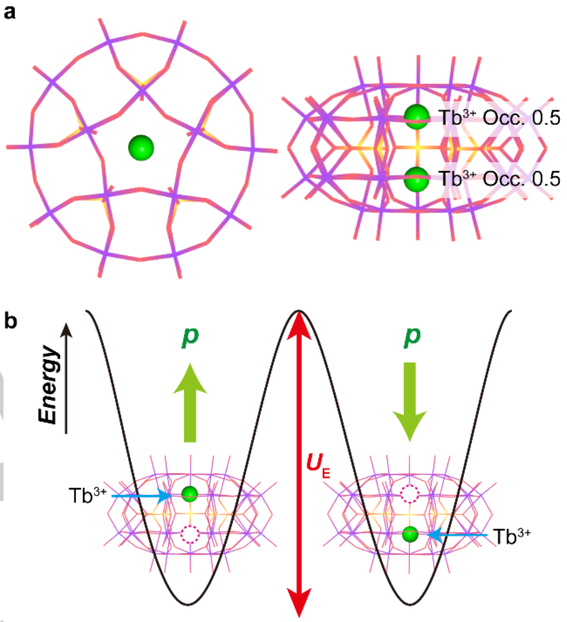

Figure 1. (a) Side and top views of $[\mathrm{Tb}^{3+}\subset\mathrm{P}_5\mathrm{W}_{30}\mathrm{O}_{110}]^{12-}$ cluster. [Colour code: green (Tb), red (O), purple (W), and yellow (P)]. Two stable terbium ion sites exist within the $[\mathrm{Tb}^{3+}\subset\mathrm{P}_5\mathrm{W}_{30}\mathrm{O}_{110}]^{12-}$ structure, and their occupancies are 0.5 each.[5] (b) Schematic showing of the double-well potential structure of the dipole moment with energy barrier U_E between two stable terbium sites in $[\mathrm{Tb}^{3+}\subset\mathrm{P}_5\mathrm{W}_{30}\mathrm{O}_{110}]^{12-}$. The direction of the dipole moment (p) is determined by the localisation site of the terbium ion.

Preyssler-type polyoxometalates (POMs) of the general formula $[\mathrm{M}^{n+}\subset\mathrm{P}_5\mathrm{W}_{30}\mathrm{O}_{110}]^{(15-n)-}$, which were discovered in 1970,[3] form one of several high-symmetry clusters of early transition metals (such as molybdenum and tungsten) with a metal-oxide framework template by either tetrahedral or octahedral ions. It has a flattened-ball architecture with five internal PO_4 tetrahedra sandwiched by corner-shared octahedra of two $\mathrm{W}_{15}\mathrm{O}_{45}$ hemispheres, which are themselves edge-shared through ten pairs of octahedral.[4] The internal space can accommodate one metal ion; however, crystallographic studies have consistently reported two equivalent positions for the metal ions due to structural symmetry (Figure 1a).[5] When two energetically stable ion sites can be interconverted through an energy barrier (U_E), this double-well potential implements the reversal of the electric dipole moment by thermal energy and electric fields (Figure 1b).

We found that for $\mathrm{K}_{12}[\mathrm{Tb}^{3+}\subset\mathrm{P}_5\mathrm{W}_{30}\mathrm{O}_{110}]$ ($[\mathrm{Tb}^{3+}\subset\mathrm{P}_5\mathrm{W}_{30}]$), the terbium ion moves randomly between the two sites at high temperature, and it localises at either site without a structural phase transition as the temperature is decreased. From the temperature- and frequency-dependent dielectric properties, the wide frequency range of dielectric dispersions can be attributed to

---

[a] Dr. C. Kato, R. Machida, R. Maruyama, Prof. Dr. K. Inoue, Dr. S. Nishihara*
Department of Chemistry
Hiroshima University
1-3-1, Kagamiyama, Higashi-hiroshima 739-8526, Japan
E-mail: snishi@hiroshima-u.ac.jp
[b] Dr. R. Tsunashima
Graduate School of Science and Engineering
Yamaguchi University
1377-1, Yoshida, Yamaguchi 753-8512, Japan
[c] Prof. Dr. X. –M. Ren
State Key Laboratory of Materials-Oriented Chemical Engineering, College of Chemistry and Molecular Engineering, and College of Materials Science & Engineering
Nanjing Teck University
Nanjing 210009, P. R. China
[d] Prof. Dr. X. –M. Ren
State Key Laboratory of Coordination Chemistry
Nanjing University
Nanjing 210023 P. R. China
[e] Prof. Dr. M. Kurmoo
Institut de Chimie de Strasbourg, CNRS-UMR7177
Université de Strasbourg
4 rue Blaise Pascal 67070, Strasbourg, France
[f] Prof. Dr. M. Kurmoo, Prof. Dr. K. Inoue, Dr. S. Nishihara
Chirality Research Center
Hiroshima University
1-3-1, Kagamiyama, Higashi-hiroshima 739-8526, Japan
[g] Prof. Dr. K. Inoue, Dr. S. Nishihara
Institute for Advanced Materials Research
Hiroshima University
1-3-1, Kagamiyama, Higashi-hiroshima 739-8526, Japan

Supporting information for this article is given via a link at the end of the document.

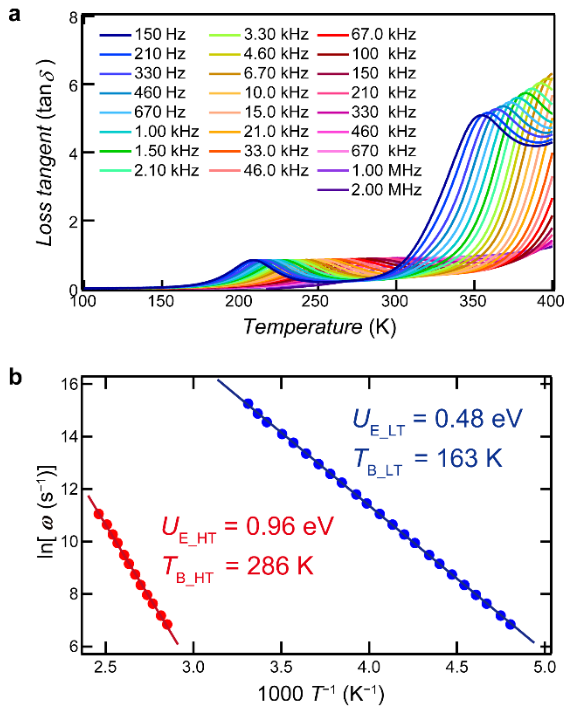

Figure 2. (a) Temperature and frequency (*f*) dependence of loss tangent (tan*δ*) for $[\mathrm{Tb}^{3+}\subset\mathrm{P}_5\mathrm{W}_{30}]$. The result shows no first-order phase transition in the measurable temperature range, while peaks depending on the frequencies in each high- and low-temperature region contribute to thermally activated relaxation processes. (b) Arrhenius plot generated from frequencies (*ω*) and peak temperature corresponding to tan*δ* for $[\mathrm{Tb}^{3+}\subset\mathrm{P}_5\mathrm{W}_{30}]$ in high- (red) and low-temperature (blue) relaxation process. The solid lines represent linear fittings to estimate U_E and T_B for the two relaxation processes (see text).

terbium-ion movement in the molecule. This compound exhibits ferroelectric-like behaviour but without long-range dipole ordering, as can be seen from the hysteretic electric-field dependence of polarisation (*P*–*E*) and temperature-dependent polarisation (*P*–*T*). These behaviours originate from a single POM molecule, as confirmed by the above electric measurements for samples of POM molecules dispersed in a polymer.

Single crystals of $[\mathrm{Tb}^{3+}\subset\mathrm{P}_5\mathrm{W}_{30}]$ were prepared according to previously reported methods.[6] The crystal belongs to the centro-symmetric orthorhombic space group *Pnma* above 100 K. Each molecule in the unit cell is crystallographically equivalent, and the terbium-ion movement is parallel to the *b*-axis (Figure S1). The as-grown crystals crumble upon exposure to air under ambient conditions owing to the loss of water of crystallisation. Thus, dielectric, *P*–*E*, and *P*–*T* measurements were performed on pellet samples of $[\mathrm{Tb}^{3+}\subset\mathrm{P}_5\mathrm{W}_{30}]$ dehydrated after keeping at 353 K for 4 h in vacuum.

Figure 2a shows the temperature and frequency dependence of the loss tangent (tan*δ*), while Figure S2 shows those of the real (ε') and imaginary (ε'') parts of the dielectric constant of $[\mathrm{Tb}^{3+}\subset\mathrm{P}_5\mathrm{W}_{30}]$. These measurements were performed by employing the four-probe method in the temperature range of 100–400 K and frequency (*f*) range of 150 Hz–2.00 MHz. The results do not indicate a phase transition in the measured temperature region. However, this compound exhibits two thermally activated relaxation processes corresponding to the variation in tan*δ*, which correspond to peaks depending on the frequency in the high- and low-temperature regions. We suggest that one of the relaxation processes is terbium-ion movement within each individual molecule. The Arrhenius plot of the peak temperature and frequency ($\omega = 2\pi f$) of tan*δ* curves in the high-temperature region yields the energy barrier $U_\mathrm{E\_HT}$ of 0.96 eV and blocking temperature $T_\mathrm{B\_HT}$ of 286 K (f = 0.1 Hz). The corresponding values for the low-temperature relaxation process are $U_\mathrm{E\_LT}$ = 0.48 eV and $T_\mathrm{B\_LT}$ = 163 K (f = 0.1 Hz), respectively (Figure 2b).

Clear polarisation hysteresis is observed in *P*–*E* measurements using a positive-up-negative-down (PUND) method, which eliminates non-ferroelectric contributions such as leakage current, at room temperature for $[\mathrm{Tb}^{3+}\subset\mathrm{P}_5\mathrm{W}_{30}]$ at 0.100 Hz (Figure 3a and S3). The temperature dependence of spontaneous polarisation yields a polarisation maximum of 2.1 μC·cm^{-2} for a maximum electric field of ±2.0 kV·cm^{-1} at 300 K, which exactly corresponds to $T_\mathrm{B\_HT}$ estimated from the dielectric measurements (Figure 3b). These results indicate that the terbium-ion movement within the molecule relates to the high-temperature relaxation process. The saturation polarisation, measured at 290 K, is estimated to be approximately 6 μC·cm^{-2} for a maximum electric field of ±4.0 kV·cm^{-1} (Figure 3c and S4). This value is greater than that of 1.4 μC·cm^{-2} calculated based on the crystal structure of $[\mathrm{Tb}^{3+}\subset\mathrm{P}_5\mathrm{W}_{30}]$ with the random orientation factor, and it is comparable to that of a typical ferroelectric material, triglycine sulphate.[7] We also performed *P*–*E* measurements at ~$T_\mathrm{B\_LT}$ to investigate the origin of the low-temperature relaxation process. The *P*–*E* curves exhibit a small banana-shaped loop in the narrow temperature region around $T_\mathrm{B\_LT}$, which typically appears with increasing conductance (See Figure S5).[8] Thus, we assumed that the vibrations of the counter cations or electronic effects in the sample influence the low-temperature relaxation process.

The *P*–*T* measurements of $[\mathrm{Tb}^{3+}\subset\mathrm{P}_5\mathrm{W}_{30}]$ were performed by heating the sample at a rate of 0.5 K·min^{-1} in zero electric field after cooling in an electric field of ±0.55 kV·cm^{-1} below 250 K, and the spontaneous polarisation values *P* (μC·cm^{-2}) were obtained through integration of the observed pyroelectric currents. Figure 3d shows the temperature dependence of the normalised polarisation P/P_100K (normalised to the absolute polarisation values P_100K at 100 K). The P/P_100K curve begins to decrease at 200 K and becomes zero at approximately 290 K. Moreover, for the same measurements employing a faster heating rate of 2.0 K·min^{-1}, the *P*–*T* curve shifts to a higher temperature. This result indicates two important material characteristics: (a) this compound does not exhibit a definite critical temperature corresponding to ferroelectric phase transition, and (b) the observed *P*–*E* hysteresis appears to correspond to the slow relaxation of the dipole in each molecule.

To demonstrate that these characteristics originate from a single-molecule property, we measured the above-mentioned properties using a sample in which POM molecules were dispersed in polymethylmethacrylate (PMMA) polymer, PMMA@$[\mathrm{Tb}^{3+}\subset\mathrm{P}_5\mathrm{W}_{30}]$. The sample was obtained by drying a chloroform solution containing PMMA and TBA-$[\mathrm{Tb}^{3+}\subset\mathrm{P}_5\mathrm{W}_{30}]$. We employed the latter, prepared by the metathesis of $[\mathrm{Tb}^{3+}\subset\mathrm{P}_5\mathrm{W}_{30}]$ and tetrabutylammonium (TBA) salt, because it is soluble in

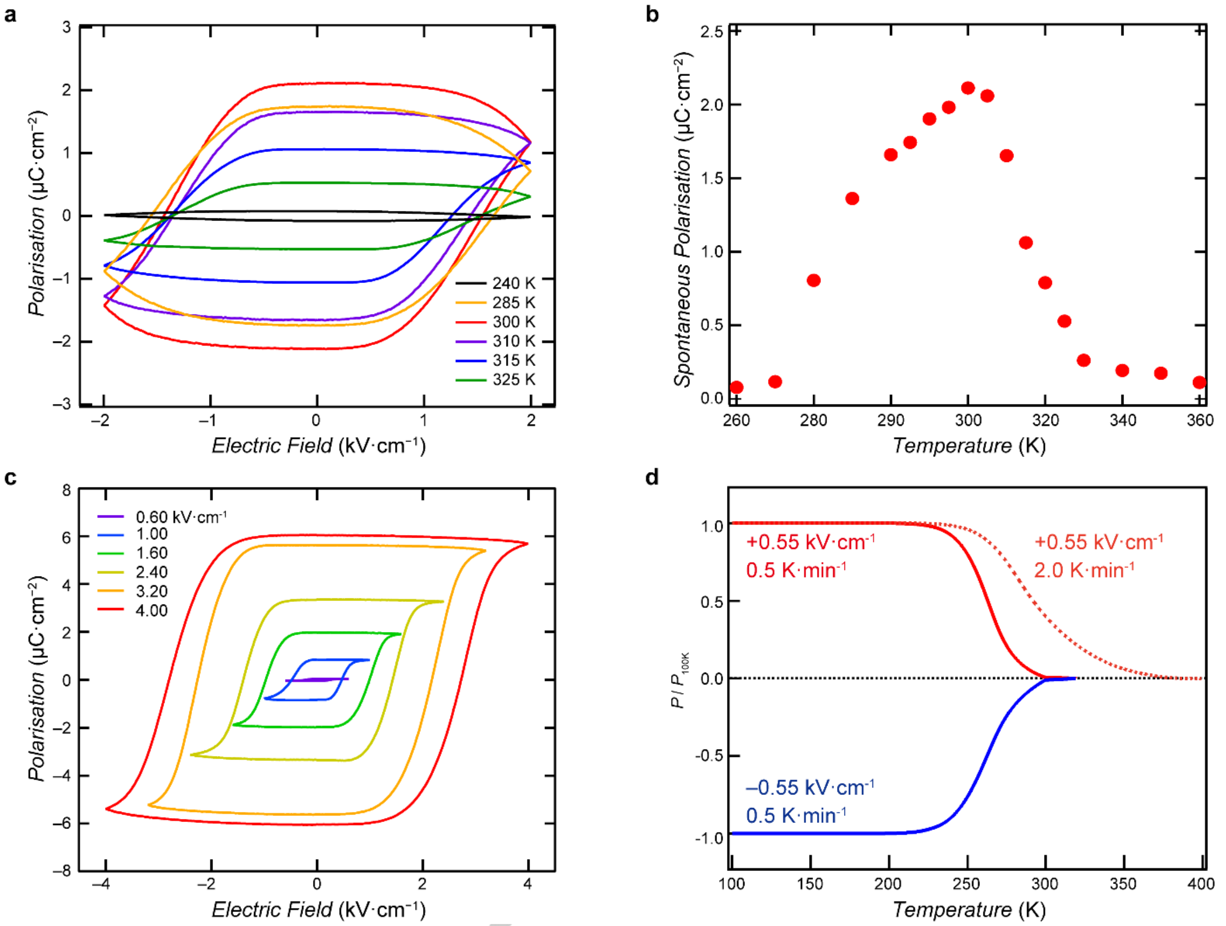

Figure 3. (a) Temperature dependence of P–E hysteresis loops and (b) spontaneous polarisation (Ps) of $[\mathrm{Tb}^{3+}\subset\mathrm{P_5W_{30}}]$ under maximum applied field of ±2.0 kV·cm^{-1} at 0.100 Hz. (c) Hysteresis loops depending on applied field at 290 K. (d) Temperature dependence of the spontaneous polarisation $P/P_{100\mathrm{K}}$ of $[\mathrm{Tb}^{3+}\subset\mathrm{P_5W_{30}}]$ for heating rates of 0.5 (solid lines) and 2.0 K·min^{-1} (dotted line) in a zero-electric field after electric-field cooling at ±0.55 kV·cm^{-1} below 250 K, where $P/P_{100\mathrm{K}}$ is normalised by the absolute polarisation value $P_{100\mathrm{K}}$ at 100 K.

organic solvents. The P–E curve for PMMA@$[\mathrm{Tb}^{3+}\subset\mathrm{P_5W_{30}}]$ obtained using the PUND method shows a small P–E hysteresis (Figure S6). Furthermore, the P–T curves clearly show a pyroelectric current at an electric field of 6.9 kV·cm^{-1}. Moreover, the P–T curve at a heating rate of 2.0 K·min^{-1} shifted to a higher temperature compared to that at 0.5 K·min^{-1} corresponding to the pellet samples of $[\mathrm{Tb}^{3+}\subset\mathrm{P_5W_{30}}]$ (Figure S7). These experiments indicate that the ferroelectric-like behaviour originates from an individual POM molecule and is not a collective effect.

To establish this association to SME clearly, we performed the dielectric measurements for $\mathrm{K_{12}[Er^{3+}\subset P_5W_{30}O_{110}]}$ ($[\mathrm{Er}^{3+}\subset\mathrm{P_5W_{30}}]$),[6] which has structures isomorphous to $[\mathrm{Tb}^{3+}\subset\mathrm{P_5W_{30}}]$. The temperature dependence of tanδ for $[\mathrm{Er}^{3+}\subset\mathrm{P_5W_{30}}]$ showed behaviours similar to that of $[\mathrm{Tb}^{3+}\subset\mathrm{P_5W_{30}}]$, in which two thermally activated frequency dispersions appeared in low- and high-temperature regions (Figure S8). In the low-temperature region, the estimated energy barrier of 0.48 eV was almost equal to that for $[\mathrm{Tb}^{3+}\subset\mathrm{P_5W_{30}}]$, while an energy barrier of 0.87 eV was obtained in the high-temperature region for $[\mathrm{Er}^{3+}\subset\mathrm{P_5W_{30}}]$, which depends on the encapsulated lanthanide ion species. These results support our inference that the frequency dispersion in the high-temperature region is attributed to the ion motions in the POM molecules. We can simply suggest that a smaller ion radius (0.923 Å for Tb^{3+} and 0.881 Å for Er^{3+} [9]) leads to a lower energy barrier to reverse the polarisation ($U_{\mathrm{E\_HT}}$ = 0.96 and 0.87 eV for the $\mathrm{Tb}^{3+}$and Er^{3+} compounds, respectively).

Similar single-molecule systems called single-molecule magnets (SMMs)[10] and single-ion magnets (SIMs)[11] have been reported. In SMMs/SIMs, the energy barrier U_{M} for spin reversal, which is related to T_{B}, scales with a negative-axial zero-field splitting parameter D and the square of the total spin (S) of the molecule.[12] This double-well potential allows for the slow relaxation of magnetisation. This relaxation process is observed as frequency dispersion in temperature-dependent alternating current (AC) magnetic susceptibility measurements, and magnetic hysteresis is obtained below T_{B} without magnetic long-range ordering.[10],[12],[13] While the discovery of SMMs/SIMs is promising for application to ultra-high-density information storage, its low operating temperature (blocking temperature T_{B}) hinders its practical use. In fact, the T_{B} of an SIM barely reached 60 K very recently.[14] The stagnation of T_{B} growth in SMMs/SIMs results from the unusual difficulty in controlling U_{M} via the parameters D and S. On the other hand, SMEs are greatly advantageous compared to these systems because not only U_{E} but also its performance and switching rate can be easily controlled by varying the size, valence, coordination ability, and so on of the included ion.

In conclusion, through measurements of the temperature dependence of the dielectric properties, *P–E*, and *P–T* of a Preyssler-type POM containing a terbium ion, we showed that this compound is an SME, which exhibits electric hysteresis at temperatures above room temperature. In addition, the blocking temperature and energy barrier for the reversal of the electric dipole moment are significantly higher than those of SMMs. We believe that our findings will enable rapid advancements in the field of single-molecule ferroic materials. Moreover, this SME material is practically realisable because it is prepared using simple wet processes and has good solubility in water and organic solvents. It remains to be seen if this material exhibits the macroscopic quantum tunnelling effect as in SMMs.[15] We believe the wide range of promising properties of single-molecule Preyssler-type POMs can be practically utilized to develop quantum devices and computers operating at room temperature.[16]

Experimental Section

Single-crystal X-ray structural analysis: All the diffraction measurements were performed using a Bruker SMART APEX II ULTRA diffractometer with a Turbo X-ray source (TXS) fine-focus rotating anode (MoKα radiation, λ = 0.71073 Å) and multilayer optics. The data collection was performed with a Japan Thermal Engineering TC-190CP-CS N_2-gas-flow cryostat. The structures were resolved by direct methods (SHELXS-97) and refined using the full-matrix least-squares method on F^2 with SHELXL-97 [17]. The single crystal for X-ray diffraction measurements was stored in silicon oil because it dehydrates rapidly in air.

Sample preparation for electric measurements: Pellet samples (0.169–0.370 mm in thickness and 1.46–133 mm^2 in area) for electronic measurements were moulded by applying pressure to the powdered samples. For the dielectric measurements, two gold wires (25 µm in diameter) were attached to one electrode prepared on each side of the pellet sample by gold paste. Similarly, one wire was attached on each side of the pellet for *P–T* measurements. *P–E* measurements were performed using a handmade stainless-steel cell and by inserting the pellet between the cell electrodes.

Dielectric measurements: The pellet sample attached with four electric wires was stored at 100–400 K in a temperature-controlled cryostat with a helium compressor; all the electric wires connected to the sample were then plugged to an electric cable connected to the cryostat exterior. The complex dielectric constant was measured using the four-probe method by heating the sample at a rate of 0.5 K·min^{-1} in vacuum. The measurements were performed in a frequency range of 150 Hz–2.00 MHz with an Agilent E4980A LCR meter under a 2.00 V AC electric field.

P–E measurements: The *P–E* measurements were performed using a handmade stainless-steel cell in the cryostat. The cell comprised a Teflon hollow cylinder and paired stainless-steel electrodes. The pellet or polymer sample was set in the cylinder hollow between the top and bottom electrodes. The *P–E* hysteresis loop was recorded at a voltage sweep range of either 0.100 or 1.00 Hz on a Sawyer-Tower circuit (Precision LCII, Radiant Technologies, Inc.). For determining the electric-field dependence of *P–E* measurements of $[\mathrm{Tb}^{3+}\subset\mathrm{P}_5\mathrm{W}_{30}]$, we could not apply an electric field greater than 4.0 kV·cm^{-1} because of short-circuiting. For all *P–E* measurements, we employed a positive-up-negative-down (PUND) method, which is often used to eliminate non-ferroelectric contributions such as leakage current (e.g., in Ref. [18]).

P–T measurements: *P–T* measurements for the pellet samples were also performed in the cryostat. The pyroelectric current was measured with an electrometer (Keithley 6517A) under zero electric field by heating the sample at a rate of either 0.5 or 2.0 K·min^{-1} after a poling procedure under an electric field at a temperature below 250 K to avoid short-circuiting. The *P–T* curves were then obtained by integrating the pyroelectric current. For the sample of POM molecules dispersed in PMMA polymer, the poling electric field was +6.9 kV·cm^{-1}, and the heating limit was 320 K because the PMMA polymer softens with heat.

Acknowledgements

This study was supported by JSPS KAKENHI Grant Numbers JP16H04223, JP16K14101, JP24350095, and JP25220803; the Joint Research Project between JSPS and the National Science Foundation of China (NSFC); and JSPS Core-to-Core Program, A. Advanced Research Networks. This work was also performed under the aegis of the Canon Science Promotion Foundation, Murata Science Foundation, Casio Science Promotion Foundation, and the Cooperative Research Program of ‘Network Joint Research Centre for Materials and Devices’. MK is also funded by CNRS, France.

Keywords: Polyoxometalates • Molecular electronics • Molecular devices

[1] a) C. Busche, L. Vila-Nadal, J. Yan, H. N. Miras, D. -L. Long, V. P. Georgiev, A. Asenov, R. H. Pedersen, N. Gadegaard, M. M. Mirza, D. J. Paul, J. M. Poblet, L. Cronin, *Nature* **2014**, *515*, 545-549; b) M. Mannini, F. Pineider, P. Sainctavit, C. Danieli, E. Otero, C. Sciancalepore, A. M. Talarico, M.-A. Arrio, A. Cornia, D. Gatteschi, R. Sessoli, *Nat. Mater.* **2009**, *8*, 194-197.

[2] a) Ye, Z. –G, Handbook of Advanced Dielectric, Piezoelectric and Ferroelectric Materials: Synthesis, Properties and Applications, Woodhead Publishing Limited, CRC Press, New York, **2008**; b) J. F. Scott, *Science* **2007**, *315*, 954–959; c) T. Akutagawa, H. Koshinaka, D. Sato, S. Takeda, S. –I. Noro, H. Takahashi, R. Kumai, Y. Tokura, T. Nakamura, *Nat. Matter.* **2009**, *8*, 342-347.

[3] C. Preyssler, *Bull. Soc. Chim. Fr.* **1970**, *1*, 30–36.

[4] M. H. Alizadeh, S. P. Harmalker, Y. Jeannin, J. Martin-Frère, M. T. J. Pope, *J. Am. Chem. Soc.* **1985**, *107*, 2662–2669.

[5] J. A. Fernández, X. López, C. Bo, C. de Graaf, E. J. Baerends, J. M. Poblet, *J. Am. Chem. Soc.* **2007**, *129*, 1244–12253.

[6] I. Creaser, M. C. Heckel, R. J. Neitz, M. T. Pope, *Inorg. Chem.* **1993**, *32*, 1573–1578.

[7] B. T. Matthias, C. E. Miller, J. P. Remeika, *Phys. Rev.* **1956**, *104*, 849–850.

[8] J. F. Scott, *J. Phys.: Condens. Matter.* **2008**, *20*, 021001/1–2.

[9] F. A. Cotton, G. Wilkinson, Advanced Inorganic Chemistry, John Wiley & Sons, Ltd., New York, **1999**.

[10] R. Sessoli, D. Gatteschi, A. Caneschi, M. A. Novak, *Nature* **1993**, *365*, 141–143.

[11] N. Ishikawa, M. Sugita, T. Ishikawa, S. Koshihara, Y. Kaizu, *J. Am. Chem. Soc.* **2003**, *125*, 8694–8695.

[12] M.A. Novak, W. S. D. Folly, J.P. Sinnecker, S. Soriano, *J. Magn. Magn. Mater.* **2005**, *294*, 133–140.

[13] D. Gatteschi, R. Sessoli, J. Molecular Nanomagnets, Oxford University Press, Oxford, **2006**; b)C. Paulsen, J. -G. Park, B. Barbara, R. Sessoli, A. Caneschi, *J. Magn. Magn. Mater.* **1995**, *140–144*, 379–380 (1995).

[14] C. Goodwin, F. Ortu, D. Reta, N. Chilton, D. Mills, *Nature* **2017**, *548*, 439–442 (2017).

[15] L. Thomas, F. Lionti, R. Ballou, D. Gatteschi, R. Sessoli, B. Barbara, *Nature 383*, 145–147 (1996).

[16] a) M. N. Leuenberger, D. Loss, *Nature* **2001**, *410*, 789–793; b) 21. S. Thiele, F. Balestro, R. Ballou, S. Klyatskaya, M. Ruben, W. Wernsdorfer, *Science* **2014**, *344*, 1135–1138.

[17] G. M. Sheldrick, *Acta Cryst.* **2008**, *A64*, 112–122.

[18] S. Horiuchi, Y. Tokuranag, G. Giovannetti, S. Picozzi, H. Ito, R. Shimano, R. Kumai, Y. Tokura, *Nature* **2010**, 463, 789–792.

Entry for the Table of Contents

COMMUNICATION

We report single-molecule electric polarization switching in a Preyssler-type polyoxometalate (POM) cluster, which exhibits all the characteristics of ferroelectricity but without long-range dipole ordering. The phenomenon affords bi-stability due to the two potential positions of localisation of a terbium ion (Tb^{3+}) trapped within the enclosed POM.

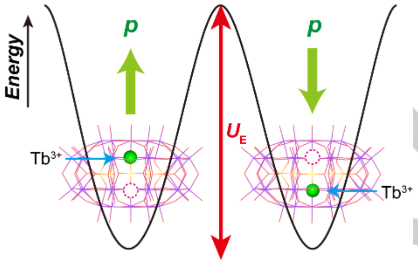

*Chisato Kato, Ryo Machida, Rio Maruyama, Ryo Tsunashima, Xiao-Ming Ren, Mohamedally Kurmoo, Katsuya Inoue, Sadafumi Nishihara**

Page No. – Page No.

Giant Hysteretic Single-Molecule Electric Polarisation Switching above Room Temperature